Overactive endocannabinoid signaling impairs apolipoprotein E-mediated clearance of triglyceride-rich lipoproteins

Maxwell A. Ruby*, Daniel K. Nomura†, Carolyn S. S. Hudak†, Lara M. Mangravite*, Sally Chiu*, John E. Casida†‡, and Ronald M. Krauss*‡

*Children's Hospital Oakland Research Institute, Oakland, CA 94609; and †Environmental Chemistry and Toxicology Laboratory, Department of Environmental Science, Policy and Management, University of California, Berkeley, CA 94720-3112

Contributed by John E. Casida, University of California, Berkeley, CA, July 25, 2008 (sent for review June 9, 2008)

The endocannabinoid (EC) system regulates food intake and energy metabolism. Cannabinoid receptor type 1 (CB1) antagonists show promise in the treatment of obesity and its metabolic consequences. Although the reduction in adiposity resulting from therapy with CB1 antagonists may not account fully for the concomitant improvements in dyslipidemia, direct effects of overactive EC signaling on plasma lipoprotein metabolism have not been documented. The present study used a chemical approach to evaluate the direct effects of increased EC signaling in mice by inducing acute elevations of endogenously produced cannabinoids through pharmacological inhibition of their enzymatic hydrolysis by isopropyl dodecylfluorophosphonate (IDFP). Acute IDFP treatment increased plasma levels of triglyceride (TG) (2.0- to 3.1-fold) and cholesterol (1.3- to 1.4-fold) in conjunction with an accumulation in plasma of apolipoprotein (apo)E-depleted TG-rich lipoproteins. These changes did not occur in either CB1-null or apoE-null mice, were prevented by pretreatment with CB1 antagonists, and were not associated with reduced hepatic apoE gene expression. Although IDFP treatment increased hepatic mRNA levels of lipogenic genes (*Srebp1* and *Fas*), there was no effect on TG secretion into plasma. Instead, IDFP treatment impaired clearance of an intravenously administered TG emulsion, despite increased postheparin lipoprotein lipase activity. Therefore, overactive EC signaling elicits an increase in plasma triglyceride levels associated with reduced plasma TG clearance and an accumulation in plasma of apoE-depleted TG-rich lipoproteins. These findings suggest a role of CB1 activation in the pathogenesis of obesity-related hypertriglyceridemia and underscore the potential efficacy of CB1 antagonists in treating metabolic disease.

2-arachidonoylglycerol | hypertriglyceridemia | monoaylglycerol lipase | organophosphorus | cannabinoid receptor

Obesity elicits a cluster of interrelated disorders, termed the "metabolic syndrome," that increases the risk of cardiovascular disease (1). Epidemiological and genetic data indicate that dysregulation of the endocannabinoid (EC) system increases adiposity in humans (2–4). Pharmacological or genetic ablation of the cannabinoid type 1 receptor (CB1) in normal mice and in diet-induced and genetic mouse models of obesity results in a transient hypophagic response mediated through the hypothalamus, but there also are prolonged effects on weight loss, adiposity, and normalization of metabolic parameters, including plasma lipids (5–11). These effects suggest that the improvement in adiposity-related measures with CB1 inactivation is not limited to reduced food intake, a major known effect of CB1 inactivation (5, 11). CB1 activation in liver increases *de novo* lipogenesis and decreases fatty acid oxidation (12, 13). High-fat diet or chronic ethanol treatment increases cannabinoid signaling tone via increased hepatic CB1 receptor density and EC levels leading to CB1-mediated hepatic steatosis (12, 13). These observations raise the possibility that aberrant EC signaling mediates development of obesity-related metabolic disturbances.

The EC system consists of the cannabinoid receptors, the endocannabinoids (ECs), and the enzymes responsible for their synthesis and breakdown (14, 15). CB1 is a G protein-coupled membrane receptor that transmits its response via $G_{i/o}$ protein-mediated reduction in adenylate cyclase activity (14). The ECs anandamide and 2-arachidonoylglycerol (2-AG) are produced locally by *N*-acyl phosphatidylethanolamine phospholipase D and by diacylglycerol lipase, respectively (14, 15). Signaling is terminated primarily by enzymatic breakdown of anandamide by fatty acid amide hydrolase (FAAH) and of 2-AG by monoacylglycerol lipase (MAGL) (14–18).

Important specific CB1 antagonists are the pharmaceutical rimonabant, with a 4-chlorophenyl substituent, and its 4-iodophenyl analog AM251. In four large human trials (19–23), rimonabant at 20 mg/day resulted in clinically significant and prolonged reductions in body weight and waist circumference and improved cardiometabolic risk factors associated with obesity. There were significant improvements in plasma triglyceride (TG) and high-density lipoprotein (HDL) cholesterol that could not be accounted for fully by the expected effects of caloric restriction and weight loss, suggesting a direct and beneficial effect of CB1 blockade on lipid metabolism.

Inhibition of MAGL and/or FAAH offers an attractive approach to study the primary effects of elevated EC signaling on specific metabolic parameters. The organophosphorus compound isopropyl dodecylfluorophosphonate (IDFP) inhibits both MAGL and FAAH *in vivo* in mice, raises brain 2-AG and anandamide levels by more than 10-fold, and elicits full-blown cannabinoid behavior (18). CB1-mediated effects of IDFP can be clearly differentiated from off-target actions by reversal with a specific CB1 antagonist and by their absence in CB1−/− mice (18). This study determined the effects of IDFP-induced overactive EC signaling and CB1 agonism on lipid metabolism, independent of adiposity or food intake. We found that elevation of EC levels was sufficient to increase plasma TG levels in conjunction with apolipoprotein (apo)E depletion of TG-rich lipoproteins and reduced plasma TG clearance.

Results

IDFP Inhibits MAGL Activity and Elevates 2-AG Levels in Liver, Muscle, and Adipose Tissue. IDFP *in vivo* (10 mg/kg, i.p., 4 h posttreatment) inhibited 2-AG hydrolytic activity in liver, skeletal muscle,

Author contributions: M.A.R. and D.K.N. contributed equally to this work; M.A.R., D.K.N., J.E.C., and R.M.K. designed research; M.A.R., D.K.N., C.S.S.H., L.M.M., and S.C. performed research; M.A.R., D.K.N., J.E.C., and R.M.K. analyzed data; and M.A.R., D.K.N., J.E.C., and R.M.K. wrote the paper.

The authors declare no conflict of interest.

‡To whom correspondence may be addressed. E-mail: ectl@nature.berkeley.edu or rkrauss@chori.org.

This article contains supporting information online at www.pnas.org/cgi/content/full/0807232105/DCSupplemental.

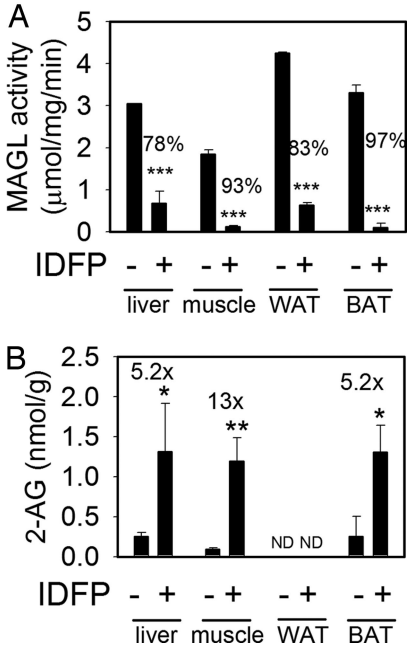

Fig. 1. IDFP inhibition of MAGL activity (*A*) and elevation of 2-AG levels (*B*) in liver, muscle, and adipose tissue. Mice were treated with DMSO or IDFP (10 mg/kg, i.p., 4 h). $n = 3–4$. BAT, brown adipose tissue; WAT, white adipose tissue.

white adipose tissue, and brown adipose tissue by 78% to 97% and raised 2-AG levels in liver, muscle, and brown adipose tissue by 5- to 13-fold (Fig. 1). 2-Oleoyl- and 2-palmitoylglycerol levels also were elevated in these tissues, but 1-oleoyl- and 1-palmitoylglycerol were less affected [supporting information (SI) Table S1].

CB1-Dependent Effects of IDFP on Plasma Lipid Levels and Lipoprotein Profiles. IDFP significantly increased plasma TG (2.0- to 3.1-fold) (Fig. 2*A*) and cholesterol levels (1.3- to 1.4-fold) (Fig. 2*B*) and very low-density lipoprotein (VLDL) mass (2.1-fold) (Fig. 2*C*) 4 h after administration. Each of these effects was ablated completely by pretreatment with the CB1 antagonist AM251 and was absent in CB1−/− mice (Fig. 2). HDL cholesterol levels were unaffected (Table S2). The increased TG and cholesterol levels were largely in the plasma VLDL fraction, accompanied by small alterations in particle composition resulting mainly from reduced protein content (Table S3). The synthetic CB1 agonist WIN55212–2 also raised plasma TG levels and VLDL mass (Fig. S1). An FAAH-selective inhibitor (URB597) (15) did not show these effects, indicating that anandamide elevation alone was not responsible (Fig. S1). Rimonabant also reversed IDFP-induced hypertriglyceridemia (Fig. S2), suggesting a mechanism and potency similar to that of AM251.

CB1-Dependent Effects of IDFP on Hepatic Lipogenic Gene Expression and TG Secretion. IDFP increased hepatic expression of the genes for both sterol regulatory element binding protein-1c and fatty acid synthase, changes that were prevented by AM251 and were not found in CB1−/− mice (Fig. S3). TG secretion then was measured by Poloxamer-407 injection to inhibit lipase-mediated TG-rich lipoprotein clearance (24). No significant differences were observed between the DMSO, IDFP, and AM251 plus IDFP treatment groups (Fig. 3). Also the lack of effect of WIN55212–2 (Fig. 3) excluded increased hepatic or intestinal TG-rich lipoprotein secretion as a contributing factor to the plasma TG elevation.

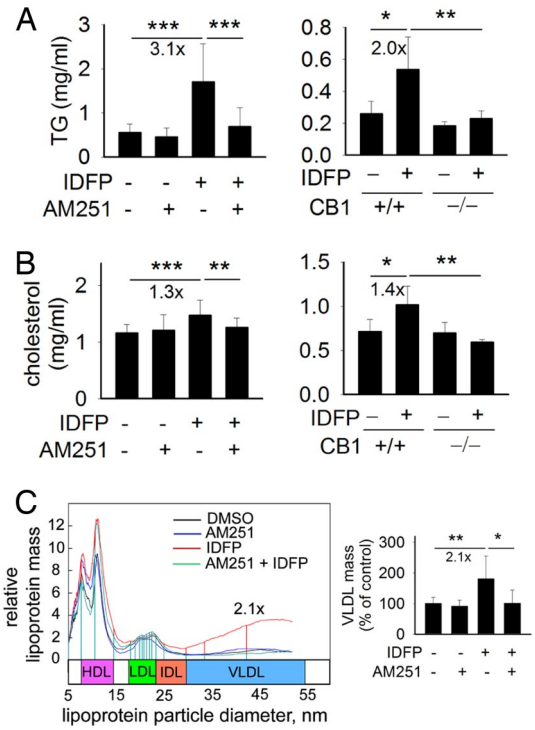

Fig. 2. CB1-dependent effects of IDFP on plasma TG (*A*) and cholesterol (*B*) levels and lipoprotein profiles (*C*). Mice were treated with DMSO or IDFP (10 mg/kg, i.p., 4 h) alone or 15 min following AM251 (10 mg/kg, i.p.). $n = 5–21$.

CB1-Dependent Effects of IDFP on TG Clearance. Clearance of an intravenously administered Intralipid TG emulsion was impaired by treatment with IDFP, an effect completely blocked by pretreatment with AM251 (Fig. 4) and reproduced by WIN55212–2 administration (Fig. S4). IDFP treatment increased postheparin lipoprotein lipase activity, a response also prevented by AM251 pretreatment (Fig. S5).

CB1-Dependent Effects of IDFP on Apolipoprotein Content of TG-Rich Lipoproteins. Consistent with the effects of IDFP treatment on plasma TG concentrations, there were substantial increases in VLDL apoB100 and apoB48 (Fig. 5). However, there was no concurrent increase in VLDL apoE with IDFP treatment,

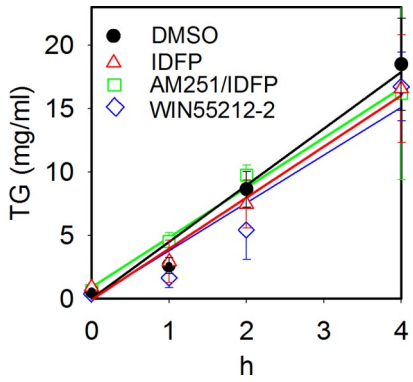

Fig. 3. CB1-dependent effects of IDFP on hepatic TG output. Mice were treated with DMSO, IDFP, or AM251 plus IDFP as in Fig. 2, or with WIN55212–2 (10 mg/kg, i.p.). Poloxamer-407 (1000 mg/kg, i.p.) was administered 15 min after the other compounds. The TG production rates for DMSO, IDFP, AM251 plus IDFP, or WIN55212–2 were 187 ± 27, 178 ± 47, 188 ± 60, and 184 ± 39 μmol/kg/h, respectively. $n = 5$.

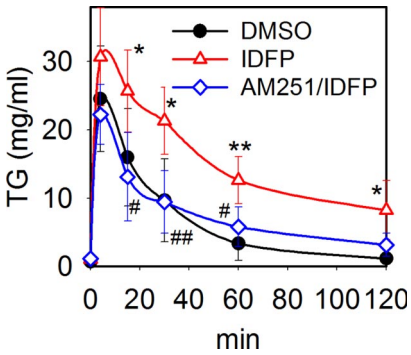

Fig. 4. CB1-dependent effects of IDFP on plasma TG clearance. Intralipid 20% TG emulsion (150 μl) was administered i.v. 2 h after DMSO, IDFP, or AM251 plus IDFP as in Fig. 2. The rates of clearance were 0.56 mg/ml/min for DMSO, 0.36 mg/ml/min for IDFP, and 0.48 for AM251 plus IDFP. Significance is expressed as *, $P < 0.05$ and **, $P < 0.01$ between DMSO and IDFP and as #, $P < 0.05$ and ##, $P < 0.01$ between IDFP and AM251 plus IDFP-treatment groups. $n = 4–6$.

resulting in a reduced ratio of apoE to apoB. IDFP treatment also increased the apoAI content of the VLDL fractions. Similar changes in apolipoproteins, although of much lesser magnitude, were observed in the intermediate-density lipoprotein (IDL) and low-density lipoprotein (LDL) fractions (Fig. S6). Interestingly, HDL apoE content was increased by 3.1-fold in IDFP-treated mice, and this increase was negated by AM251 (Fig. S6). Hepatic transcript levels of apoE, apoAI, apoAV, and apoCIII were unchanged (Table S4).

ApoE-Dependent Effects of IDFP on Plasma Lipid Levels. A possible role for apoE depletion in mediating the increase of TG-rich lipoproteins induced by overactive EC signaling was tested by studies in apoE-null mice (25) and age- and sex-matched apoE+/+ controls. IDFP elicited 2.1- and 1.1-fold increases in plasma TG and cholesterol levels, respectively, in apoE+/+ mice, whereas it had no significant effect in apoE−/− mice (Fig. 6). Differences in apolipoprotein and lipid composition between apoE+/+ and apoE−/− mice in the combined VLDL and IDL fraction were similar to those observed in VLDL from mice treated with DMSO or IDFP. (Fig. 5; Fig. S7).

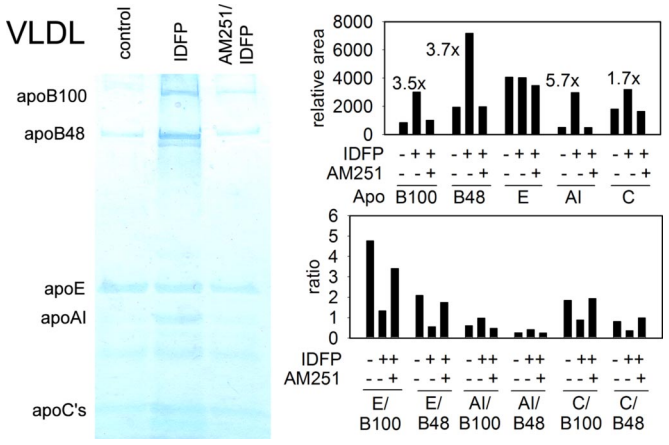

Fig. 5. CB1-dependent effects of IDFP on apolipoproteins in the VLDL fraction. Mice were treated as in Fig. 2, and plasma from 10 mice was pooled for analysis. VLDL apolipoprotein composition was quantitated based on Commassie staining. IDL, LDL, and HDL apolipoprotein compositions are shown in Fig. S6. Lipid composition of the VLDL fraction is given in Table S3.

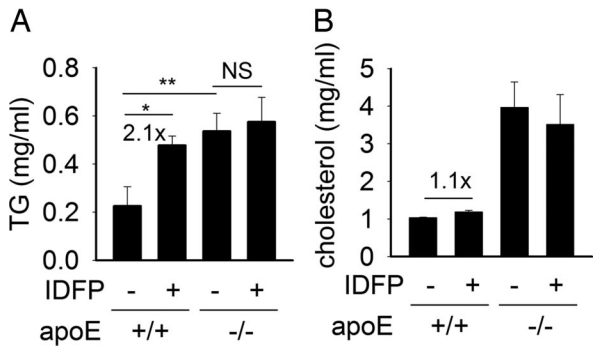

Fig. 6. ApoE-dependent effects of IDFP on plasma TG (*A*) and cholesterol (*B*) levels. ApoE+/+ and −/− mice were treated with DMSO or IDFP (10 mg/kg, i.p., 4 h). $n = 3–4$.

Discussion

The involvement of the EC system in the regulation of plasma lipid and lipoprotein metabolism has been demonstrated in several clinical trials by the effects of treating obese patients with the CB1 antagonist rimonabant (19–23). These effects include reductions in plasma TG and small LDL particles and increases in HDL cholesterol. A major determinant of these changes is the weight loss resulting from reduced caloric intake, but post hoc analysis suggests that this weight loss is not sufficient to explain the full magnitude of the drug's effects (23). To determine the contribution of elevated EC signaling to plasma lipid and lipoprotein metabolism, independent of food intake or adiposity, we used IDFP to raise systemic levels of 2-AG acutely by inhibiting its hydrolysis.

The present study establishes that overactive EC signaling is sufficient to elicit hypertriglyceridemia acutely in a CB1-dependent manner characterized by accumulation of TG-rich lipoproteins. Hypertriglyceridemia can result from increased hepatic production or decreased catabolism of TG-rich lipoproteins, which undergo lipolytic processing to remnant particles that can be cleared from plasma through apoE-mediated receptor endocytosis. Hepatic *de novo* lipogenic gene transcript levels were elevated upon overactive EC signaling, as observed also under chronic ethanol administration (13). However, this elevation was not paralleled in our studies by increased hepatic TG secretion, indicating that the TG elevation resulted from CB1-dependent impairment in TG clearance. The finding of reduced plasma removal of Intralipid supports this conclusion. Like chylomicrons, TG emulsions such as Intralipid rapidly acquire apolipoproteins, including the lipoprotein lipase activator apoCII and apoE, and hepatic uptake of whole particles has been visualized by electron microscopy (26, 27). Despite the presence of apoCII and susceptibility to *in vitro* lipase activity, emulsion droplets similar to those found in Intralipid are removed from plasma with little preceding lipolysis (28). This finding, in combination with our observation that postheparin lipoprotein lipase activity was increased by IDFP in a CB1-dependent manner, indicates that reduced lipolysis was not responsible for the impaired TG clearance induced by increased CB1 signaling. However, alterations in other factors that determine lipoprotein lipase functional activity (e.g., apoCII, apoCIII, fasting-induced adipose factor) or localization of LPL on the capillary surface could potentially cause a defect in lipolysis that would not be apparent in postheparin plasma lipase activity (29, 30).

We propose that defective clearance of TG-rich lipoproteins in IDFP-treated mice results from decreased apoE-mediated whole-particle uptake. This mechanism might explain previous reports that CB1−/− mice have reduced TG levels despite the

MEDICAL SCIENCES

stimulatory effect of CB1 activation on adipose tissue lipoprotein lipase activity (5, 12). Indeed, IDFP-induced CB1 signaling resulted in both apoE depletion and apoAI enrichment of VLDL particles. ApoAI normally is associated with HDL particles but has been observed on TG-rich lipoproteins in the genetic absence of apoE. ApoE plays a multifunctional role in intravascular and cellular lipid metabolism, primarily as a ligand for the seven identified members of the LDL receptor family and for cell surface heparin proteoglycans (31, 32). Although apoE is expressed throughout the body, circulating apoE largely originates from the liver, where both newly synthesized and recycled apoE is secreted (33). The ablation of IDFP-induced hypertriglyceridemia in apoE−/− mice indicates that CB1 activation impairs apoE-mediated clearance of TG-rich lipoproteins. It is interesting that IDFP-induced increases in plasma TG values in +/+ mice reached levels similar to those in apoE−/− mice. Despite high basal TG levels, apoE−/− mice can undergo still further increases in TG as a result of enhanced secretion or impaired lipolytic clearance (34, 35). As shown here for IDFP-treated wild-type mice, apoE−/− mice have similarly high concentrations of apoAI in native apoB-containing lipoproteins and accumulation in plasma of apoB48 particles that rely solely on apoE for receptor-mediated clearance. Additionally, TG-rich lipoproteins in apoE−/− mice turn over slowly and are enriched in sphingomyelin at the expense of phosphatidylcholine (36). These differences may alter their susceptibility to lipolysis, as influenced by the endocannabinoid system, compared with TG-rich lipoproteins in +/+ mice. Moreover, given differential gene expression in the apoE−/− mice, we cannot rule out the possibility that indirect mechanisms account for the loss of the IDFP hyperlipidemic effects in apoE−/− mice (37).

IDFP-treated mice do not develop the severe hypercholesterolemia characteristic of apoE−/− mice, perhaps because of the short treatment period coupled with the slower turnover of cholesterol-rich compared with TG-rich lipoproteins. Alternatively, depletion of apoE may not be sufficient to cause hypercholesterolemia; individuals with the apoE2/E3 genotype have decreased concentrations of apoE3 protein but display decreased LDL cholesterol levels (38). The coupling of apoE depletion in TG-rich lipoproteins with increased apoE content of HDL particles suggests that CB1 activation may alter the partitioning of secreted apoE or cause a conformational change in apoE on HDL or VLDL resulting in altered equilibration between these apoE pools. The mechanism by which CB1 activation alters apoE distribution remains to be elucidated.

Although hepatic CB1 activation probably is the target of our observed effects, we cannot exclude centrally mediated actions upon peripheral tissues because brain EC levels are elevated as well (18). However, the ablation of TG elevation in apoE−/− mice even in the presence of full-blown cannabinoid behavioral effects (observed in this study in IDFP-treated apoE+/+ and −/− mice and ref. 18) strongly argues that the CB1-mediated hypertriglyceridemia and apoE effects are mediated peripherally. The development of peripheral CB1 antagonists that do not cross the blood-brain barrier and tissue-specific CB1−/− mouse models (13) will aid in addressing this issue.

IDFP effects on TG metabolism could result from its inhibition of MAGL and/or FAAH. Notably, fibrogenic stimuli elevate hepatic 2-AG, whereas a high-fat diet elevates anandamide levels, and both ECs are implicated in pathogenesis of hepatic steatosis (12, 13). Although we show here that FAAH inhibition alone (by URB597) is not sufficient to elicit acute hypertriglyceridemia, evaluation of the specific effects of 2-AG will require development of a selective MAGL inhibitor or a MAGL−/− mouse model. Moreover, IDFP off-targets, such as hormone-sensitive lipase, neuropathy target esterase, carboxylesterase-N, and alpha/beta hydrolases 3 and 6 (18), may potentiate the EC actions observed here. However, the complete reversal of IDFP effects by pharmacological (AM251 and rimonabant) or genetic (in CB1−/− mice) ablation of CB1 unequivocally ascribes the metabolic abnormalities to the EC system.

Our short-term studies in fasted mice show that CB1-mediated reduction in plasma TG clearance does not require alterations in food intake or body weight. The findings, however, do not define the contribution of this mechanism to longer-term effects of CB1 activation, particularly in the context of changes in adiposity, or to its role in humans. For example, increased hepatic secretion of TG-rich lipoproteins might result from chronic CB1-induced activation of hepatic lipogenic pathways with high fat diet or ethanol intake (12, 13). Moreover, our studies do not identify direct effects of CB1 activation on HDL metabolism, as might be expected given the weight-independent effects of rimonabant on HDL levels in humans (21–23). Because the turnover time of HDL lipoproteins is much greater than that of TG-rich lipoproteins, such effects may require a longer duration of CB1 activation. Other factors, such as cholesteryl ester transfer protein activity, which is absent in mice (39), may be required also. It is of interest, however, that the apoE content of HDL was increased by CB1 activation, and this increase, coupled with VLDL enrichment of apoAI, might lead to changes in HDL production or clearance that would be apparent with a longer duration of IDFP treatment. Unfortunately long-term IDFP treatment is not an option because of probable delayed non-CB1-dependent central nervous system toxicity (40).

ECs are elevated before the onset of obesity (10), implicating hyperactive EC signaling as a cause of metabolic disease rather than a consequence. Despite encouraging clinical data, rimonabant failed to gain Food and Drug Administration approval because of psychiatric side effects, illustrating both the promise of targeting the EC system for treatment of obesity-related metabolic disturbances and the need to understand better the basic biology and pharmacology involved. It may then be possible to develop CB1 antagonists that limit adverse psychological side effects while achieving the desired metabolic endpoints.

Methods

Animals. Swiss Webster mice were from Harlan Laboratories. CB1+/+ and −/− breeding pairs were obtained from Andreas Zimmer and Carl Lupica (41). ApoE−/− mice (25) and C57/Bl6 +/+ controls were obtained from Jackson Laboratories. All mice were 6–8 weeks of age, male, and weighed 18–23 g, with the exception of CB1−/− mice (17 ± 2 g). They were fasted for 4 h, were treated i.p. at 1 μl/g with DMSO or test compounds dissolved in DMSO, and were killed at the indicated times. All experiments used Swiss Webster mice unless specifically stated otherwise (i.e., +/+ or −/−). Mice lightly anesthetized with isoflurane for injection of IDFP and AM251 were fully recovered within 2 min.

Chemicals. Sources for the chemicals were as follows: lipid standards from Alexis Biochemicals and Sigma; AM251 and WIN55212–2 from Tocris Cookson Inc .; rimonabant from AK Scientific; Poloxamer-407 from BASF Corporation; Intralipid TG emulsion from Sigma; and [^{3}H]triolein from Perkin-Elmer. IDFP was synthesized in the Berkeley laboratory (40).

MAGL Activity and Monoacylglycerol Levels. MAGL activity was determined by measuring 2-AG hydrolysis using GC-MS (18). Tissue homogenates in 5 ml of 50 mM Tris buffer (pH 8.0) containing 1 mM EDTA and 3 mM $MgCl_2$ were centrifuged at 1000 *g*. Supernatant protein (50 μg) was incubated with 100 μM 2-AG in Tris/EDTA/$MgCl_2$ buffer (500 μl) for 1 h at 37°C then extracted with 1 ml ethyl acetate containing 10 nmol of the internal standard 1-dodecylglycerol. After phase separation, 70% of the upper organic layer was recovered, evaporated under nitrogen, and derivatized by *N*,*O*-bis(trimethylsilyl)trifluoroacetamide (200 μl) for 30 min at room temper-

ature with sonication. The trimethylsilyl derivatives (1 μl aliquot) were separated on a DB-XLB fused-silica capillary column (30 m $\times$ 0.25 mm $\times$ 25 μm) using a temperature program of 100° to 280°C and detected by electron impact ionization at 70 eV with an ion source temperature of 250°C. A mass selective detector was used for single-ion monitoring to quantitate individual lipids. MAGL activity was based on the formation of arachidonic acid (with endogenous arachidonic acid levels subtracted) normalized for tissue weight and internal standard. Monoacylglycerol levels in tissues were determined as described previously (18). Briefly, tissues were weighed and homogenized in a mixture of 3 ml 100 mM phosphate buffer (pH 7.4) and 3 ml ethyl acetate containing 10 nmol of internal standard. The ethyl acetate phase was recovered, and after workup the trimethylsilyl derivatives were analyzed by GC-MS as indicated previously.

Plasma Lipids and Lipoproteins. Plasma was used for determination of lipid and lipoprotein profiles. Total TG and cholesterol were analyzed by enzymatic end-point measurements using enzyme reagent kits (Sigma) with HDL cholesterol concentration determined by measurement directly after polyethylene glycol-mediated precipitation of apoB (42). For ion mobility analysis of lipoprotein particle concentrations (43), one part plasma was incubated with four parts albumin-binding agent (reactive green 19 dextran); this mixture was layered on top of deuterium oxide and was spun in an ultracentrifuge to isolate the lipoproteins. The lipoprotein fraction was injected into the ion mobility instrument, which utilizes an electrospray to create an aerosol. The particles then were passed through a differential mobility analyzer coupled to a condensation particle counter, where particle diameter and quantity were determined.

TG Production Rate and Clearance. The hepatic TG production rate was assessed by measuring temporal increases in plasma TG during inhibition of clearance using poloxamer-407 (24) administered i.p. at 1000 mg/kg 15 min following DMSO, IDFP, AM251 plus IDFP, or WIN55212–2 treatment. TG values were determined for plasma samples collected at 0, 1, 2, and 4 h as described previously. The TG production rate was calculated as the difference in plasma TG levels over the 4-h interval. TG clearance was determined by i.v. infusion of Intralipid (150 μl) and measuring plasma TG levels at 0, 4, 15, 30, 60, and 120 min thereafter. TG clearance rate was calculated from the difference in plasma TG between 4 and 30 min.

Lipoprotein Fractionation. VLDL, IDL, LDL, and HDL fractions were separated from pooled plasma by sequential density ultracentrifugation (44). ApoB100, B48, E, and C in each fraction were quantified by measuring Coomassie band intensity after separation by denaturing gradient gel electrophoresis. Lipid compositions were determined as described previously.

Statistical Analyses. Results are presented as mean $\pm$ standard deviation. One-way and two-way analysis of variance was used to test significance of treatment effects and interactions with genotypes, respectively. Post hoc analysis (Student's unpaired *t* test) examined significance of individual treatment and/or genotype effects. Significance is given as $P < 0.05$, $P < 0.01$, and $P < 0.001$. All analyses were performed using JMP version 7.0 (SAS Institute Inc.).

For more information, please see *SI Methods*.

ACKNOWLEDGMENTS. We thank our University of California, Berkeley colleagues Roger Issa and Lindsey Jennings for help in the animal studies and Rita Nichiporuk and Ulla Andersen for advice in the mass spectrometry analyses. We also thank J. Casey Geaney of Children's Hospital Oakland Research Institute for assistance with plasma lipoprotein measurements. We are indebted to Yoffi Segall of the Israel Institute of Biological Research, Ness-Ziona, for initial synthesis and repreparation of IDFP for this study. This work was supported by the Department of Atherosclerosis Research at Children's Hospital Oakland Research Institute (R.M.K.), National Institutes of Health Grant ES008762 (J.E.C.), and the University of California Toxic Substances Research and Teaching Program (D.K.N.).

1. Lakka H-M, *et al.* (2002). The metabolic syndrome and total and cardiovascular disease mortality in middle-aged men. *JAMA* 288:2709–2716.
2. Blüher M, *et al.* (2006). Dysregulation of the peripheral and adipose tissue endocannabinoid system in human abdominal obesity. *Diabetes* 55:3053–3060.
3. Engeli S, *et al* (2005). Activation of the peripheral endocannabinoid system in human obesity. *Diabetes* 54:2838–2843.
4. Sipe JC, Waalen J, Gerber A, Beutler E (2005) Overweight and obesity associated with a missense polymorphism in fatty acid amide hydrolase (FAAH). *Int J Obes* 29:755–759.
5. Cota D, *et al.* (2003). The endogenous cannabinoid system affects energy balance via central orexigenic drive and peripheral lipogenesis. *J Clin Invest* 112:423–431.
6. Ravinet Trillou C, *et al.* (2003). Anti-obesity effect of SR141716, a CB1 receptor antagonist, in diet-induced obese mice. *Am J Physiol Regul Integr Comp Physiol* 284:R345–353.
7. Ravinet Trillou C, Delgorge C, Menet C, Arnone M, Soubrié P (2004) CB1 cannabinoid receptor knockout in mice leads to leanness, resistance to diet-induced obesity and enhanced leptin sensitivity. *Int J Obes* 28:640–648.
8. Jbilo O, *et al.* (2005). The CB1 receptor antagonist rimonabant reverses the diet-induced obesity phenotype through the regulation of lipolysis and energy balance. *FASEB J* 19:1567–1569.
9. Di Marzo V, *et al.* (2001). Leptin-regulated endocannabinoids are involved in maintaining food intake. *Nature* 410:822–825.
10. Starowicz KM, *et al.* (2008). Endocannabinoid dysregulation in the pancreas and adipose tissue of mice fed with a high-fat diet. *Obesity* 16:553–563.
11. Colombo G, *et al.* (1998). Appetite suppression and weight loss after the cannabinoid antagonist SR 141716. *Life Sci* 63:PL113–117.
12. Osei-Hyiaman D, *et al.* (2005). Endocannabinoid activation at hepatic CB1 receptors stimulates fatty acid synthesis and contributes to diet-induced obesity. *J Clin Invest* 5:1298–1305.
13. Jeong W-I, *et al.* (2008). Paracrine activation of hepatic CB_1 receptors by stellate cell-derived endocannabinoids mediates alcoholic fatty liver. *Cell Metab* 7:227–235.
14. Piomelli D (2003) The molecular logic of endocannabinoid signaling. *Nat Rev Neurosci* 4:873–884.
15. Ahn K, McKinney MK, Cravatt BF (2008) Enzymatic pathways that regulate endocannabinoid signaling in the nervous system. *Chem Rev* 108:1687–1707.
16. Cravatt BF, *et al.* (2001). Supersensitivity to anandamide and enhanced endogenous cannabinoid signaling in mice lacking fatty acid amide hydrolase. *Proc Natl Acad Sci USA* 98:9371–9376.
17. Blankman JL, Simon GM, Cravatt BF (2007) A comprehensive profile of brain enzymes that hydrolyze the endocannabinoid 2-arachidonoylglycerol. *Chem Biol* 14:1347–1356.
18. Nomura DK, *et al.* (2008). Activation of the endocannabinoid system by organophosphorus nerve agents. *Nat Chem Biol* 4:373–378.
19. Després J-P, Golay A, Sjöström L (2005) Effects of rimonabant on metabolic risk factors in overweight patients with dyslipidemia. *N Engl J Med* 353:2121–2134.
20. Pi-Sunyer FX, *et al.* (2006). Effect of rimonabant, a cannabinoid-1 receptor blocker, on weight and cardiometabolic risk factors in overweight or obese patients: RIO-North America: A randomized controlled trial. *JAMA* 295:761–775.
21. Scheen AJ, *et al.* (2006). Efficacy and tolerability of rimonabant in overweight or obese patients with type 2 diabetes: A randomised controlled study. *Lancet* 368:1660–1672.
22. Van Gaal LF, *et al.* (2005). Effects of the cannabinoid-1 receptor blocker rimonabant on weight reduction and cardiovascular risk factors in overweight patients: 1-year experience from the RIO-Europe study. *Lancet* 365:1389–1397.
23. Van Gaal LF, *et al.* (2008). Long-term effect of CB_1 blockade with rimonabant on cardiometabolic risk factors: Two year results from the RIO-Europe study. *Eur Heart J* 29:1761–1771.
24. Millar JS, *et al.* (2005). Determining hepatic triglyceride production in mice: Comparison of Poloxamer 407 with Triton WR-1339. *J Lipid Res* 46:2023–2028.
25. Piedrahita JA, Zhang SH, Hagaman JR, Oliver PM, Nobuyo M (1992) Generation of mice carrying a mutant apolipoprotein E gene inactivated by gene targeting in embryonic stem cells. *Proc Natl Acad Sci USA* 89:4471–4475.
26. Vilaro S, Llobera M (1988) Uptake and metabolism of Intralipid by rat liver: An electron-microscopic study. *J Nutr* 118:932–940.
27. Tong MF, Kuksis A (1986) Effect of different neutral phospholipids on apolipoprotein binding by artificial lipid particles in vivo. *Biochem Cell Biol* 64:826–835.
28. Hultin M, Carneheim C, Rosenqvist K, Olivecrona T (1995) Intravenous lipid emulsions: Removal mechanisms as compared to chylomicrons. *J Lipid Res* 36:2174–2184.
29. Beigneux AP, *et al.* (2007). Glycosylphosphatidylinositol-anchored high density lipoprotein-binding protein 1 plays a critical role in the lipolytic processing of chylomicrons. *Cell Metab* 5:279–291.
30. Mandard S, *et al.* (2006). The fasting-induced adipose factor/angiopoietin-like protein 4 is physically associated with lipoproteins and governs plasma lipid levels and adiposity. *J Biol Chem* 281:934–944.
31. Meir KS, Leitersdorf E (2004) Atherosclerosis in the apolipoprotein E-deficient mouse: A decade of progress. *Arterioscler Thromb Vasc Biol* 24:1006–1014.
32. Ishibashi S, Herz J, Maeda N, Goldstein JL, Brown MS (1994) The two-receptor model of lipoprotein clearance: Tests of the hypothesis in ''knockout'' mice lacking the low density lipoprotein receptor, apolipoprotein E, or both proteins. *Proc Natl Acad Sci USA* 91:4431–4435.
33. Hereen J, Beisiegal U, Grewal T (2006) Apolipoprotein E recycling: Implications for dyslipidemia and atherosclerosis. *Arterioscler Thromb Vasc Biol* 26:442–448.
34. Ebara T, Ramakrishnan R, Steinar G, Shachter NS (1997) Chylomicronemia due to apolipoprotein CIII overexpression in apolipoprotein E-null mice. Apolipoprotein CIII-induced hypertriglyceridemia is not mediated by effects on apolipoprotein E. *J Clin Invest* 99:2672–2681.
35. Conde-Knape K, Bensadoun A, Sobel JH, Cohn JS, Shachter NS (2002) Overexpression of apoC-1 in apoE-null mice: Severe hypertriglyceridemia due to inhibition of hepatic lipase. *J Lipid Res* 43:2136–2145.

36. Jeong T-S, *et al.* (1998). Increased sphingomyelin content of plasma lipoproteins in apolipoprotein E knockout mice reflects combined production and catabolic defects and enhances reactivity with mammalian sphingomyelinase. *J Clin Invest* 101:905–912.
37. Ma Y, Malbon CC, Williams DL, Thorngate FE (2008) Altered gene expression in early atherosclerosis is blocked by low level apolipoprotein E. *PLoS ONE* 3:e2503.
38. Bennet AM, *et al.* (2007). Association of apolipoprotein E genotypes with lipid levels and coronary risk. *JAMA* 298:1300–1311.
39. Joia S, Cole TG, Kitchens RT, Pfleger B, Schonfeld G (1990) Genetic heterogeneity of lipoproteins in inbred strains of mice: Analysis by gel-permeation chromatography. *Metabolism* 39:155–160.
40. Segall Y, Quistad GB, Sparks SE, Nomura DK, Casida JE (2003) Toxicological and structural features of organophosphorus and organosulfur cannabinoid CB1 receptor ligands. *Toxicol Sci* 76:131–137.
41. Zimmer A, Zimmer AM, Hohman AG, Herkenham M, Bonner TI (1999) Increased mortality, hypoactivity, and hypoalgesia in cannabinoid CB1 receptor knockout mice. *Proc Natl Acad Sci USA* 96:5780–5785.
42. Briggs CJ, Anderson D, Johnson P, Deegan T (1981) Evaluation of the polyethylene glycol precipitation method for estimation of-high density lipoprotein cholesterol. *Ann Clin Biochem* 18:177–181.
43. Caulfield MP, *et al.* (2008). Direct determination of lipoprotein particle sizes and concentrations by ion mobility analysis. *Clin Chem* 54:1307–1316.
44. Qiu S, *et al.* (1998). Metabolism of lipoproteins containing apolipoprotein B in hepatic lipase-deficient mice. *J Lipid Res* 39:1661–1668.